ELSEVIER

Journal of Alloys and Compounds 275–277 (1998) 123–126

Journal of ALLOYS AND COMPOUNDS

On the 22–23 K superconducting phase in the Y–Pd–B–C system

E. Tominez[a,*], P. Berger[b], E. Alleno[a], B. Décamps[a], G. Schiffmacher[a], M. Bohn[c], C. Godart[a]

[a]*CNRS, UPR 209, place A. Briand, 92195 Meudon Cedex, France*
[b]*Laboratoire Pierre Süe, CEA/CNRS, CE/SACLAY, 91191 Gif sur Yvette Cedex, France*
[c]*IFREMER, Centre de Brest, URA/CNRS 6538, 29280 Plouzané, France*

Abstract

Superconducting and non-superconducting (annealed) samples of $YPd_5B_3C_{0.35}$ have been investigated using electrical resistance and magnetization measurements, X-ray diffraction, electron diffraction with energy dispersive X-ray spectrometry and electron probe micro analysis (EPMA). In the superconducting sample, six phases were observed out of which two were clearly decomposed by annealing. Composition and unit cell of these phases were determined. The concentrations of boron and carbon are uncertain, due to the small atomic weight of these elements. Therefore, we report for the first time, nuclear probe micro analysis (NPMA) measurements. Preliminary results of NPMA are consistent with EPMA. At last, we suggest that the superconducting phase has a composition close to YPd_2B_2C and an *I*-centred tetragonal unit cell with $a=3.751(1)$ and $c=10.725(3)$ Å. © 1998 Elsevier Science S.A.

Keywords: Quaternary borocarbides (PACS number 74.72.Ny); Superconductivity; Nuclear probe micro analysis

1. Introduction

The multiphase alloy $YPd_5B_3C_{0.35}$ shows the highest superconducting transition temperature (T_c~23 K) ever observed for an intermetallic compound [1]. Annealing the sample 2 days at 900°C results in the complete loss of superconductivity. The superconducting phase has been tentatively identified in [2–4] as $YPd_2B_2C_x$ (x~1) having a tetragonal structure similar to superconducting $LuNi_2B_2C$ ($I4/mmm$, $a=3.7$–3.8 Å, $c=10.6$–10.8 Å). However, according to [5], the composition of the tetragonal superconducting phase was YPd_2BC, whereas [6] suggested a superconducting FCC-phase ($a=4.15$ Å) with a stoichiometry close to YPd_2B_2C.

The aim of this work is to characterise the superconducting phase. We report our preliminary study of the various phases present in a superconducting and a non-superconducting (annealed) sample of $YPd_5B_3C_{0.35}$, using electrical resistance and magnetization measurements, X-ray diffraction (XRD), transmission electron diffraction (TED) and energy dispersive X-ray spectrometry (EDX), electron probe micro analysis (EPMA) and nuclear probe micro analysis (NPMA). This is the first report on using the NPMA technique to investigate these materials.

2. Experimental

A sample of nominal composition $YPd_5B_3C_{0.35}$ was prepared by arc-melting the appropriate amounts of Y (99.9%), Pd (99.95%), B(99.7%) and C (99.7%). After melting, the ingot was cut in two pieces and one of them was vacuum annealed at 900°C for 2 days.

The superconducting properties of both samples were investigated by electrical resistance measurements using the four-probe method and magnetization measurements using a SQUID magnetometer in zero field cooled (ZFC) and field cooled (FC) conditions. EPMA was employed to determine the composition of the various phases present in the samples. Due to the small atomic weight of B and C, the determination of their concentrations by EPMA is uncertain. To compare with EPMA results, we also used NPMA. This technique consists in probing the sample with a microbeam of ions ($^3He^+$ with $E_p=3$ MeV, in this case) and allows the quantification of the heavy elements (Y, Pd) by Rutherford back scattering spectroscopy (RBS) and particle induced X-ray emission (PIXE) and of the light ones (B, C) by nuclear reactions. The independence of the nuclear reaction cross-sections upon the weight of the elements makes this technique quite unique for determining the concentration of light elements [7]. XRD analysis using a diffractometer with Cu Kα radiation was carried

*Corresponding author.

PII: S0925-8388(98)00288-6

out on both samples. The as-cast sample was also studied by TED coupled with EDX analysis. Thin samples were prepared by crushing under ethanol and dispersing the powder on a carbon holey film supported by a copper grid.

3. Results and discussion

3.1. Resistive and magnetic properties

Fig. 1 displays the temperature dependence of the magnetization for as-cast $YPd_5B_3C_{0.35}$ which exhibits a superconducting transition at 22.5 K. The sample shows a magnetic shielding (ZFC) of ~95% and a Meissner effect (FC) of ~10% of that expected for perfect diamagnetism, showing that the superconductivity is a bulk effect. The electrical resistance of the same material (see inset Fig. 1) presents an abrupt drop at approximately 22.5 K and a zero value near 20 K. No sign of superconductivity was detected in the annealed sample.

3.2. Electron probe micro analysis

The backscattered electron images (see Fig. 2 (a) and (b)) of as-cast and annealed $YPd_5B_3C_{0.35}$ show that the two samples contain a large number of phases. In Table 1, we have listed the various phases observed for the as-cast sample. The phases are clearly apparent except the phase B which is only distinguishable from the surrounding matrix by its slightly darker interface (see detail of Fig. 2(a)). The reproducibility of the microprobe data (standard deviation)

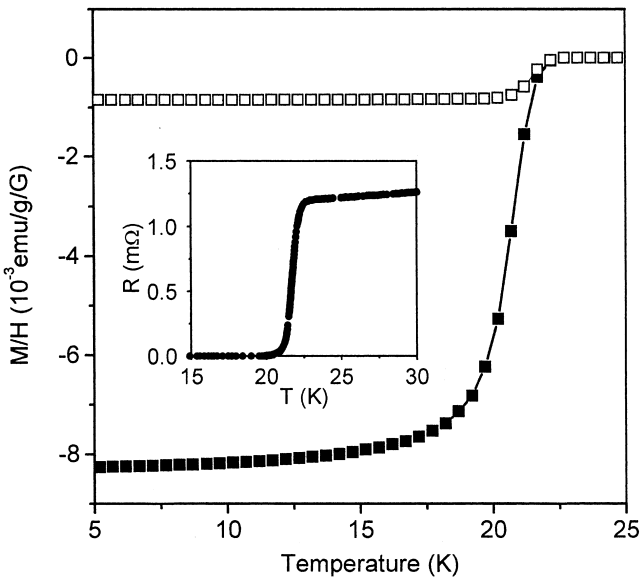

Fig. 1. Magnetic susceptibility versus temperature of the as-cast $YPd_5B_3C_{0.35}$ sample at ZFC (full squares) and FC (empty squares) conditions (measuring field of 10 G). Lines are guides for the eye. The inset shows the electrical resistance of the same sample versus temperature.

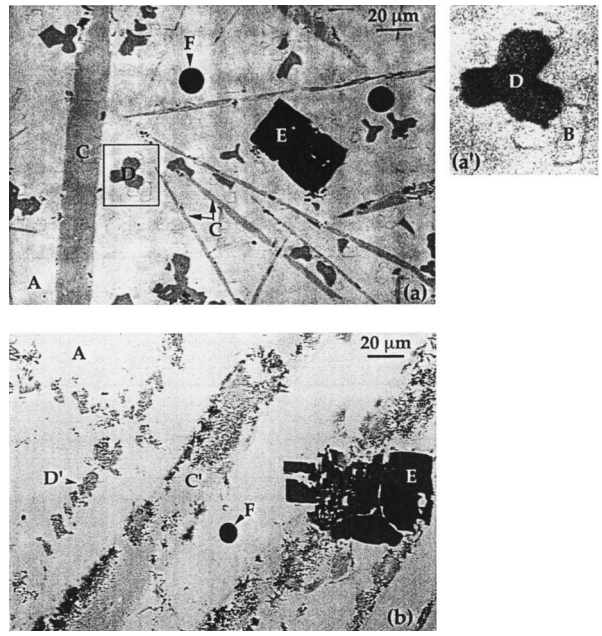

Fig. 2. Backscattered electron images of $YPd_5B_3C_{0.35}$. (a) the as-cast sample and (a′) the enlargement of boxed area in (a). (b) the annealed sample. The letters refer to the phases listed in Table 1. C′ and D′ show the traces of the phases C and D which were decomposed by annealing.

depending on the phase, is 1–2.5% for Y, 0.5–6% for Pd, 1–17% for B and ~10% for C. The volume fraction of the different phases was estimated by image analysis.

The phases A, E and F are also observed with the same composition in the annealed sample, whereas the phase B is no more visible. It may be present but without its slightly darker interface. As we can see in Fig. 2(b), the phases C and D were decomposed by annealing. Therefore, one of them can be the superconducting phase. The volume fraction of both phases is consistent with the observed Meissner effect. Phase C seems to be the most suitable candidate because of its needle-shape morphology which could allow a zero electrical resistance signal.

3.3. Nuclear probe micro analysis

Both as-cast and annealed $YPd_5B_3C_{0.35}$ samples were investigated by NPMA. Comparing our preliminary NPMA results with those obtained by EPMA (see Table 1), the boron content seems to be generally underestimated, whereas the carbon content is overestimated. Moreover, the Pd content of the matrix is deficient in comparison with the EPMA composition. This could be explained by the fact that the two techniques have different measurement parameters. Indeed, the probing depth of the ion beam is nearly equal to 3 μm, whereas we estimate the probing depth for EPMA at approximately 0.2 μm. Therefore, NPMA measurements are more representative of the bulk composition than EPMA. On the other hand, the size of the ion beam in NPMA (5×7 μm) which is

Table 1
Morphology, composition and volume fraction of the various phases observed in as-cast $YPd_5B_3C_{0.35}$

Phase code	Phase morphology	Composition (EPMA)	Volume fraction	Composition (NPMA)	Unit cell (XRD)
A	matrix	$YPd_{7.1}B_{3.9}C_x$ x<0.1	⎫70%	$YPd_{6.5}B_{3.0}C_{0.1}$	*I*-centred ortho a=8.441(4) b=8.984(5) c=16.543(8)
B	globules	$YPd_{3.0}B_{0.8}$	⎭	not measured	cubic a=4.122(1)
C	needles	$YPd_{2.0}B_{2.2}C_{0.9}$	20%	$YPd_{2.0}B_{2.0}C_{1.25}$	*I*-centred tetragonal a=3.751(1) c=10.725(3)
D	dendrites	$YPd_{1.0}B_{4.7}$	7.5%	$YPd_{1.1}B_{3.1}C_{0.1}$	cubic a=4.053(1)
E	faceted	$YB_{4.6}$	1.5%	$YB_{5.1}C_{0.1}$	tetragonal a=7.079(4) c=4.014(4)
F	spheres	$YPd_{0.3}B_{2.6}C_{5.2}$	<1%	not measured	not observed

Unit cell of the different phases detected by XRD in both as-cast and annealed $YPd_5B_3C_{0.35}$. The phases C and D are only found in the as-cast sample.

clearly larger than the EPMA probe (~1 μm^2), has the same order of magnitude as some of the phases observed in the samples. Consequently, the measured compositions could incidentally be influenced by other phases.

Additional measurements are needed to improve the experimental conditions (nature and energy of the ion beam). More details about data collection and reduction will be given in a forthcoming paper.

3.4. TED and XRD results

The superconducting $YPd_5B_3C_{0.35}$ sample was studied by TED and EDX analysis. Five different types of compositions were found with Y/Pd ratios of 1/7, 1/3, 1/2, 1/1 and 1/0 corresponding to the phases A, B, C, D and E respectively. We have not observed any grain of phase F, certainly because of its weak volume fraction. Using the crystal unit cells obtained from the TED study (see Fig. 3), most of the diffraction peaks of the X-ray diffraction patterns of the as-cast and the annealed samples (see Fig. 4), have been successfully indexed. The peaks which only appear for the superconducting sample were attributed to the two phases decomposed by annealing. The unit cells obtained from XRD (see Table 1) are consistent with those obtained from TED.

The unit cell of the matrix A is in good agreement with the one reported in [5]. In the Th–Pd–B–C system, a phase with similar composition ($ThPd_8B_3$) and same unit cell has been found [8]. The X-ray diffraction pattern of phase B is equivalent to the binary compound YPd_3 (a= 4.074 Å [9]). The a-shift may be due to the incorporation of boron. In backscattered electron images, this phase is only visible in the as-cast sample (see Section 3.2), whereas it is detected by XRD in both samples (see Fig. 4). It implies that its slightly darker interface has disappeared during the annealing treatment. The phases C and D decomposed by annealing, are only observed in the superconducting sample (see Fig. 4). Phase C shows a unit cell similar to the superconducting $LuNi_2B_2C$ with a preferential orientation of the (00l) planes, certainly due to its needle-shape morphology. Phase D adopts a cubic lattice quite similar to $ThPd_{0.65}B_{4.7}$ which was suggested to be the 21 K superconducting phase in the Th–Pd–B–C system [8]. Phase E with average composition $YB_{4.6}$ (EPMA) has a tetragonal unit cell, analogous to YB_4.

The phases C and D which are decomposed by annealing can be the superconducting phase. The volume fraction of both phases is consistent with the observed Meissner effect. Though the phase D has similar composition and unit cell to the 21 K superconducting phase in the Th–Pd–

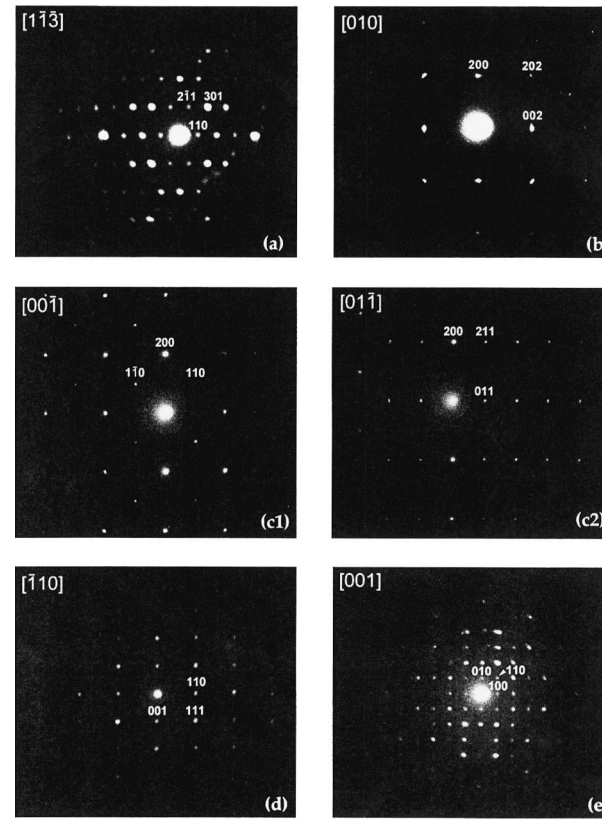

Fig. 3. Diffraction patterns of the various phases observed in the as-cast sample. (a) shows the [1$\bar{1}$3] diffraction pattern of phase A (*I*-centred orthorhombic with a=8.4, b=9.0 and c=16.7 Å). (b) shows the [010] diffraction pattern of phase B (cubic with a=4.1 Å). Only the reflections with h, k and l with the same parity are observed which indicates that phase B adopts the $AuCu_3$ structure. (c1) and (c2) show the [00$\bar{1}$] and [01$\bar{1}$] diffraction patterns of phase C (*I*-centred tetragonal with a=3.7 and c=10.7 Å). (d) shows the [$\bar{1}$10] diffraction pattern of phase D (cubic a=4.1 Å). Contrary to [5], no superstructure is observed. (e) shows the [001] diffraction pattern of phase E (tetragonal with a=7.1 and c=4.0 Å).

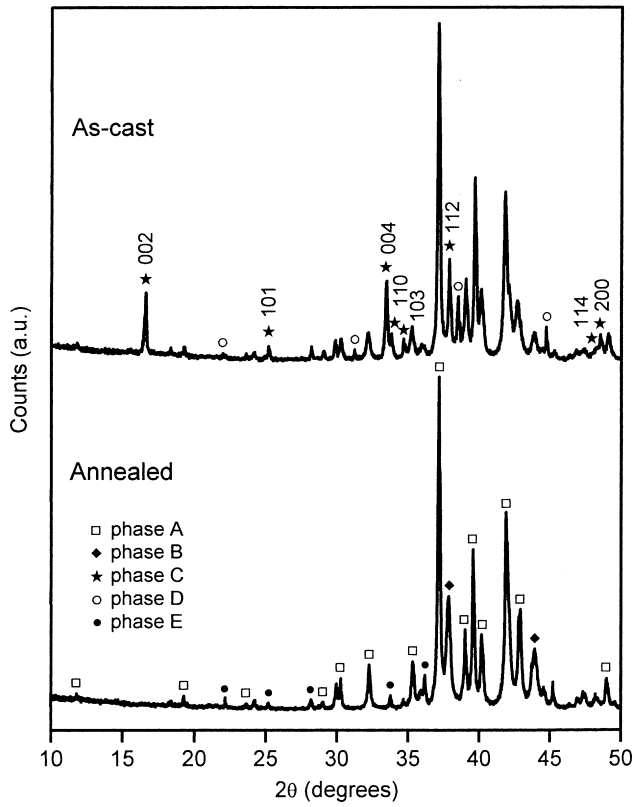

Fig. 4. Powder X-ray diffraction patterns of the as-cast and the annealed samples. Indexation is given for phase C.

B–C system, we suggest that the phase C is the superconducting phase. Indeed, we think that the structure of this phase is probably of the $LuNi_2B_2C$-type which has shown superconductivity for many isomorphous (Ni, Pt) compounds. Moreover, phase C has a needle-shape morphology which could allow the measured zero electrical resistance signal.

4. Conclusion

The study of the various phases present in the superconducting and the non-superconducting samples of $YPd_5B_3C_{0.35}$ indicates that the superconducting phase has a composition close to YPd_2B_2C and an *I*-centred tetragonal unit cell, similar to the superconducting $LuNi_2B_2C$. The five other phases contained in the as-cast sample have been characterised too. To compare with the compositions given by EPMA, nuclear probe micro analysis (NPMA) has been used on these materials for the first time. Preliminary results of NPMA are consistent with EPMA. Efforts to improve the experimental conditions are in progress.

Acknowledgements

We would like to thank C. Haut for performing the presented backscattered electron images.

References

[1] R.J. Cava, H. Takagi, B. Batlogg, H.W. Zandbergen, J.J. Krajewski, W.F. Peck Jr, R.B. van Dover, R.J. Felder, T. Siegrist, K. Mizuhashi, J.O. Lee, H. Eisaki, S.A. Carter, S. Uchida, Nature 367 (1994) 146.
[2] C.L. Jia, Y.H. Xu, M. Beyss, F. Peter, K. Urban, Physica C 229 (1994) 325.
[3] Y.Y. Sun, I. Rusakova, R.L. Meng, Y. Cao, P. Gautier-Picard, C.W. Chu, Physica C 230 (1994) 435.
[4] H. Fujii, S. Ikeda, T. Kimura, S.I. Arisawa, K. Hirata, H. Kumakura, K. Kadowaki, K. Togano, Jpn. J. Appl. Phys. 33 (1994) L590.
[5] H.W. Zandbergen, W.G. Sloof, R.J. Cava, J.J. Krajewski, W.J. Peck Jr, Physica C 226 (1994) 365.
[6] V. Ström, K.S. Kim, A.M. Grishin, K.V. Rao, J. Appl. Phys. 79 (1996) 5860.
[7] G. Demortier, Nucl. Instr. Meth. B 104 (1995) 244.
[8] H. W Zandbergen, T.J. Gortenmulder, J.L. Sarrac, J.C. Harrison, M.C. de Andrade, J. Hermann, S.H. Han, Z. Fisk, M.B. Maple, R.J. Cava, Physica C 232 (1994) 328.
[9] A.E. Dwight, R.A. Conner Jr, Acta Crystallogr. 14 (1961) 75.